2015 IEEE 26th International Symposium on Personal, Indoor and Mobile Radio Communications - (PIMRC): Fundamentals and PHY

Closed-Form Capacity Expression for Low Complexity BICM with Uniform Inputs

Ronald Nissel, Sebastian Caban and Markus Rupp
Institute of Telecommunications, TU Wien, Vienna, Austria
Email: {rnissel, scaban, mrupp}@nt.tuwien.ac.at

***Abstract*—In this paper, we derive closed-form capacity expressions for a low complexity bit-interleaved coded modulation system with uniform inputs in a Rayleigh fading channel with additive white Gaussian noise. Additionally, we include pilot-symbol assisted channel estimation in our considerations. Finding a closed-form solution is enabled by assuming quantization and that the decoder has no channel state information. The effects of these assumptions on the capacity are investigated separately. To verify our closed-form expressions and to show the applicability of our system model to real world physical channels, we perform measurements using the Vienna Wireless Testbed.**

I. Introduction

Bit-Interleaved Coded Modulation (BICM) [1], [2] is a practical, flexible and robust way of performing channel coding and allows the use of powerful binary codes, which explains its current employment in many communication standards such as wireless LAN and LTE. By assuming quantization and no Channel State Information (CSI) at the decoder, the probability density function (pdf) becomes a probability mass function (pmf) with only a limited number of possible probability values, reducing the overall complexity of a Maximum Likelihood (ML) decoder. Furthermore, such assumptions allow us to derive closed-form expressions for the capacity. Closed-form expressions are important because they provide analytical insights and allow efficient performance optimization with respect to specific parameters such as the pilot symbol design or the optimal Orthogonal Frequency Division Multiplexing (OFDM) subcarrier spacing in a doubly-selective channel. Our derivations are based on recent results of the complex Gaussian ratio distribution [3]. However, the cumulative distribution function (cdf) in [3] requires multiple functions, making it rather hard to use. By assuming a specific system model, we are able to provide a compact expression for the cdf, see Lemma 1. Our assumptions shift the capacity by a Signal-to-Noise Ratio (SNR) of approximately 3 dB. If one is interested in the ordinary capacity [1], the structure of our closed-form expressions serve as a good starting point for accurate estimations. For example, a straightforward method to estimate the ordinary capacity is a simple 3 dB SNR shift.

In practice, channel estimation plays an important role. Authors in [4] extended the BICM capacity to the case of imperfect CSI by applying Schur's complement but their evaluation was only based on Monte Carlo simulations. Our closed-form expressions also include channel estimation where, in particular, for a 4-Quadrature Amplitude Modulation (QAM) we observe that the Minimum Mean Squared Error (MMSE) channel estimation shows the same performance as perfect channel knowledge, except that the signal power is reduced by the Mean Squared Error (MSE) and the noise power increased by the MSE.

Testbed measurements are a crucial step to check if all relevant factors have been included in a specific system model. Here we do not simply rely on simulations but employ a testbed, the Vienna Wireless Testbed [5], [6], in order to verify our closed-form expressions and to show their applicability in real world physical channels.

Some authors [7] considered signal constellation shaping, i.e., non-equiprobable bit probabilities. We on the other hand follow the commonly made assumption in the BICM literature [1], [2] and assume uniform inputs (all bits have the same probability) because of its practical relevance. Capacity and mutual information then become equal and no maximization of the mutual information over the input pdf is required. Furthermore, all of our derivations are based on the ergodic capacity. See for example [8, Chapter 5] for more information about its specific implications.

II. System Model

Figure 1 represents the block diagram of our transmission system. A bit stream is encoded, bit-wise interleaved and then mapped by Gray coding to data symbols $x \in \mathcal{X}$, chosen from a 2^m-QAM signal constellation, with m being even. The channel, indicated by the gray area in the figure, consists of a multiplication and a summation, so that the received data symbols y can be written as:

$$y = hx + n, \tag{1}$$

whereas the channel $h \sim \mathcal{CN}(0, P_\mathrm{s})$ and the noise $n \sim \mathcal{CN}(0, P_\mathrm{n})$ are complex Gaussian random variables with zero mean. We assume that the data symbols x have unit power, so that the signal power is given solely by the power of h, i.e., $P_\mathrm{s} = \mathbb{E}\{hh^*\}$. The model in (1) describes, for example, OFDM systems where y represents the transmission at a certain time-frequency position.

Equalization is performed by a simple one-tap equalizer, i.e., the received data symbol y is divided by $\hat{h}$, so that the equalized received data symbol z can be expressed as:

$$z = \frac{y}{\hat{h}}. \tag{2}$$

To estimate the channel $\hat{h}$, we employ Pilot-symbol-Aided Channel Estimation (PACE), which relies on the correlation between the channel at data position and the channel at pilot positions. If there is no correlation, PACE does not work. The

978-1-4673-6782-0/15/$31.00 ©2015 IEEE

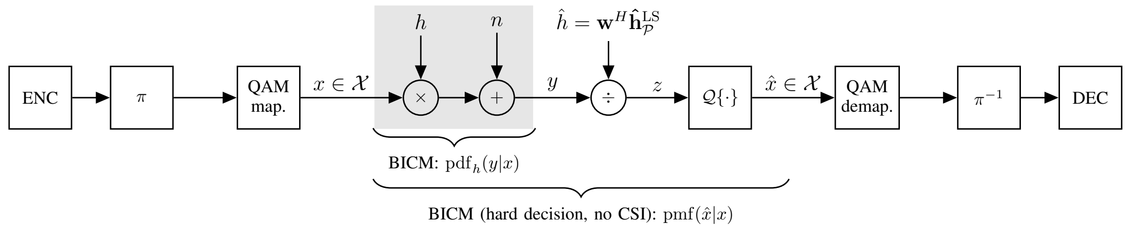

Fig. 1. Block diagram of our BICM transmission system model where π denotes bit-wise interleaving. The ordinary BICM capacity [1] applies the probability density function $\mathrm{pdf}_h(y|x)$. We, on the other hand, assume hard decision of the equalized received symbols and that the decoder has no CSI, so that the probability mass function $\mathrm{pmf}(\hat{x}|x)$ has to be used. Such approach decreases the complexity and allows us to find closed-form capacity expressions.

estimated channel $\hat{h}$ consists of an weighted average of the estimated channel at the pilot positions $\hat{\mathbf{h}}_{\mathcal{P}}^{\mathrm{LS}} \in \mathbb{C}^{|\mathcal{P}|\times 1}$:

$$\hat{h} = \mathbf{w}^H \hat{\mathbf{h}}_{\mathcal{P}}^{\mathrm{LS}}, \tag{3}$$

whereas $\mathcal{P}$ reflects the set of pilot positions and $|\mathcal{P}|$ the number of pilot symbols. The weighting vector $\mathbf{w} \in \mathbb{C}^{|\mathcal{P}|\times 1}$ can be interpreted as interpolation and can, for example, be chosen as linear, spline or MMSE interpolation. The channel estimation at the pilot positions itself is performed by a Least Squares (LS) estimation:

$$\hat{\mathbf{h}}_{\mathcal{P}}^{\mathrm{LS}} = \mathrm{diag}\{\mathbf{x}_{\mathcal{P}}\}^{-1}\mathbf{y}_{\mathcal{P}}, \tag{4}$$

where vector $\mathbf{y}_{\mathcal{P}} \in \mathbb{C}^{|\mathcal{P}|\times 1}$ represents the received data symbols at the pilot positions and $\mathbf{x}_{\mathcal{P}} \in \mathbb{C}^{|\mathcal{P}|\times 1}$ the transmitted data symbols at the pilot positions, both given in a vectorized form.

We quantize ($\mathcal{Q}\{\cdot\}$) the equalized received data symbol z, given by (2), which gives us an estimate $\hat{x} \in \mathcal{X}$ of the transmitted data symbol x. For perfect channel knowledge and no coding, this corresponds to ML estimation of x. Demapping, de-interleaving and decoding finally generates the estimated bit stream.

A perfect decoder exploits the received data symbols y as well as the perfect channel knowledge h, so that the BICM capacity with uniform inputs is given by [1]:

$$C^{\mathrm{BICM}} = m - \sum_{i=1}^{m} \mathbb{E}_{b,y,h}\left[\log_2 \frac{\sum\limits_{x\in\mathcal{X}} \mathrm{pdf}_h(y|x)}{\sum\limits_{x\in\mathcal{X}_b^i} \mathrm{pdf}_h(y|x)}\right], \tag{5}$$

with $\mathcal{X}$ being the set of a 2^m-QAM signal constellation and $\mathcal{X}_b^i$ being the subset of $\mathcal{X}$ whose label has the bit value b at position i. Similar to (5), we can calculate the capacity after the equalization step. Because the probability density functions are related by $\mathrm{pdf}_h(z|x) = |h|\,\mathrm{pdf}_h(y|x)$, the capacity is the same as in (5), thus, the equalization process does not influence the overall capacity.

A major drawback of (5) is the fact that the expectation $\mathbb{E}_{b,y,h}\{\cdot\}$ cannot be calculated in closed-form so that numerical methods, such as Monte Carlo simulations, have to be used. To circumvent this limitation we make the following assumptions:

- Hard decision: the decoder ignores y and z and uses the quantized estimates $\hat{x}$ instead.
- No CSI at the decoder: the decoder has no information about the estimated channel $\hat{h}$, although it is used for the equalization process.

Using the probability mass function (pmf), (5) then transforms to:

$$C = m - \sum_{i=1}^{m} \mathbb{E}_{b,\hat{x}}\left[\log_2 \frac{\sum\limits_{x\in\mathcal{X}} \mathrm{pmf}(\hat{x}|x)}{\sum\limits_{x\in\mathcal{X}_b^i} \mathrm{pmf}(\hat{x}|x)}\right], \tag{6}$$

with the advantages below:

- Closed-form expression: we find closed-form expressions for the capacity.
- Low complexity: because of a finite set of probabilities, large parts of the ML bit metric can be precomputed, reducing the complexity of a ML decoder.
- Channel estimation: the extension from perfect CSI to imperfect CSI is also possible in closed-form.
- Measurements: measuring the capacity becomes feasible due to a finite set of probabilities.

However, ignoring the channel estimate and the unquantized received symbols at the decoder leads to a lower capacity which constitutes the main disadvantage of our assumptions (see Section IV for more details).

III. Closed-Form Capacity Expression

In this section, we derive a closed-form expression for the BICM capacity. By splitting the expectations in (6) according to $\mathbb{E}_{b,\hat{x}}[\cdot] = \frac{1}{2}\mathbb{E}_{\hat{x}|b=0}[\cdot] + \frac{1}{2}\mathbb{E}_{\hat{x}|b=1}[\cdot]$ and using the fact that the expectations can be written as summations due to the discrete nature of $\hat{x}$, i.e., $\mathbb{E}_{\hat{x}|b=i}[\cdot] = \sum_{\hat{x}\in\mathcal{X}} \mathrm{pmf}(\hat{x}|b=i)[\cdot]$ with $\mathrm{pmf}(\hat{x}|b=i) = \frac{1}{2^{m-1}}\sum_{x\in\mathcal{X}_b^i} \mathrm{pmf}(\hat{x}|x)$, we can write (6) as:

$$C = m - \sum_{i=1}^{m}\sum_{b=0}^{1}\sum_{\hat{x}\in\mathcal{X}}\left[\frac{\sum\limits_{x\in\mathcal{X}_b^i} \mathrm{pmf}(\hat{x}|x)}{2^m} \log_2 \frac{\sum\limits_{x\in\mathcal{X}} \mathrm{pmf}(\hat{x}|x)}{\sum\limits_{x\in\mathcal{X}_b^i} \mathrm{pmf}(\hat{x}|x)}\right] \tag{7}$$

In order to express (7) in closed-form, we have to calculate the closed-form expression of the probability mass function $\mathrm{pmf}(\hat{x}|x)$. Note that, for 2^m-QAM, this pmf can take at most 2^{2m} values. However, because QAM is symmetric with respect to a $\pi/2$ rotation, there are at most $2^{2(m-1)}$ distinct probabilities. The closed-form expression for the pmf can be calculated as soon as we know the closed-form expression for the cdf of z, i.e., the received symbols after equalization. Such closed-form cdf is provided by the following Lemma :

Lemma 1: Let $h \sim \mathcal{CN}(0, P_\mathrm{s})$, $n \sim \mathcal{CN}(0, P_\mathrm{n})$ and $\hat{\mathbf{h}}_\mathcal{P}^\mathrm{LS} \sim \mathcal{CN}(\mathbf{0}, \mathbf{R}_{\hat{\mathbf{h}}_\mathcal{P}^\mathrm{LS}})$ be zero mean complex-valued Gaussian random variables and vectors. Assume further that the transmission system model is given by $y = hx + n$, that the channel is estimated by pilot symbols, i.e., $\hat{h} = \mathbf{w}^H \hat{\mathbf{h}}_\mathcal{P}^\mathrm{LS}$, with $\mathbf{w}$ being an arbitrary complex vector corresponding to the interpolation scheme, and that the cross-correlation vector $\mathbb{E}\{\hat{\mathbf{h}}_\mathcal{P}^\mathrm{LS} h^*\} = \mathbf{r}_{\hat{\mathbf{h}}_\mathcal{P}^\mathrm{LS}, h}$ is known. Conditioned on x, the probability that the real part of the complex Gaussian ratio $y/\hat{h}$ is smaller than a certain value z_R and at the same time the imaginary part smaller than z_I, reads:

$$\Pr\left(\Re\left\{\frac{y}{\hat{h}}\right\} < z_\mathrm{R} \wedge \Im\left\{\frac{y}{\hat{h}}\right\} < z_\mathrm{I} \middle| \mathrm{x} = x\right) = \frac{1}{4} + \frac{\left(z_\mathrm{R} - \Re\left\{\frac{\alpha}{\beta}x\right\}\right)\left(2\tan^{-1}\left(\frac{z_\mathrm{I} - \Im\left(\frac{\alpha}{\beta}x\right)}{\sqrt{\left(z_\mathrm{R} - \Re\{\frac{\alpha}{\beta}x\}\right)^2 + \gamma}}\right) + \pi\right)}{4\pi\sqrt{\left(z_\mathrm{R} - \Re\{\frac{\alpha}{\beta}x\}\right)^2 + \gamma}} + \frac{\left(z_\mathrm{I} - \Im\left\{\frac{\alpha}{\beta}x\right\}\right)\left(2\tan^{-1}\left(\frac{z_\mathrm{R} - \Re\left(\frac{\alpha}{\beta}x\right)}{\sqrt{\left(z_\mathrm{I} - \Im\{\frac{\alpha}{\beta}x\}\right)^2 + \gamma}}\right) + \pi\right)}{4\pi\sqrt{\left(z_\mathrm{I} - \Im\{\frac{\alpha}{\beta}x\}\right)^2 + \gamma}}, \tag{8}$$

with

$$\alpha = \mathbf{w}^H \mathbf{r}_{\hat{\mathbf{h}}_\mathcal{P}^\mathrm{LS}, h}, \tag{9}$$

$$\beta = \mathbf{w}^H \mathbf{R}_{\hat{\mathbf{h}}_\mathcal{P}^\mathrm{LS}} \mathbf{w}, \tag{10}$$

$$\gamma = \frac{P_\mathrm{n} + P_\mathrm{s}|x|^2}{\beta} - \left|\frac{\alpha}{\beta}x\right|^2. \tag{11}$$

The proof of Lemma 1 can straightforwardly be obtained by inserting our system model in the general expression of the complex Gaussian ratio distribution [3].

Of particular interest is the case when only the projection onto one axis, say the real axis, matters. Then, either z_R or z_I approaches infinity, so that the $\tan^{-1}$ terms vanish and we end up with a very compact expression. This fact will later help to find the capacity of a 4-QAM. Lemma 1 delivers the probability for arbitrary linear interpolation methods $\mathbf{w}$. Let us now consider the special case of MMSE channel estimation [9], [10]:

$$\mathbf{w}^\mathrm{MMSE} = \mathbf{R}_{\hat{\mathbf{h}}_\mathcal{P}^\mathrm{LS}}^{-1} \mathbf{r}_{\hat{\mathbf{h}}_\mathcal{P}^\mathrm{LS}, h}, \tag{12}$$

which minimizes the MSE of our channel estimation:

$$\mathbf{w}^\mathrm{MMSE} = \arg\min_\mathbf{w} \mathrm{MSE} = \arg\min_\mathbf{w} \mathbb{E}\{|h - \mathbf{w}^H \hat{\mathbf{h}}_\mathcal{P}^\mathrm{LS}|^2\}. \tag{13}$$

The variables α and β in (9) and (10) then transform to:

$$\alpha^\mathrm{MMSE} = \beta^\mathrm{MMSE} = \mathbf{w}^H \mathbf{R}_{\hat{\mathbf{h}}_\mathcal{P}^\mathrm{LS}} \mathbf{w} = P_\mathrm{s} - \mathrm{MSE}, \tag{14}$$

and γ in (11) becomes:

$$\gamma^\mathrm{MMSE} = \frac{P_\mathrm{n} + \mathrm{MSE}|x|^2}{P_\mathrm{s} - \mathrm{MSE}}. \tag{15}$$

For perfect channel knowledge, the MSE approaches zero and therefore:

$$\alpha^\mathrm{perfect} = \beta^\mathrm{perfect} = P_\mathrm{s} \tag{16}$$

and

$$\gamma^\mathrm{perfect} = \frac{P_\mathrm{n}}{P_\mathrm{s}} = \frac{1}{\mathrm{SNR}}. \tag{17}$$

Note that for MMSE channel estimation, the probability in Lemma 1 behaves the same way as for perfect channel knowledge where the signal power is lowered by the MSE and the noise power increased by $\mathrm{MSE}|x|^2$, as shown by (15) and the fact that α/β becomes one, so that Lemma 1 only depends on γ.

Lemma 1 together with (7) immediately delivers a closed-form expression for the capacity. However, the resulting expressions are quite lengthy so that we will explicitly cover only the special case of 4-QAM and perfect channel knowledge, which can easily be extended to MMSE channel estimation, as mentioned above. By a phase rotation, we can keep the conditional variable x constant, so that $\sum_{x \in \mathcal{X}} \mathrm{pmf}(\hat{x}|x) = \sum_{\hat{x} \in \mathcal{X}} \mathrm{pmf}(\hat{x}|x) = 1$, which clearly is one because the second term sums the pmf of all possible events. Again, phase rotation in combination with symmetry shows that the summation $\sum_{x \in \mathcal{X}_b^i} \mathrm{pmf}(\hat{x}|x)$ can only take two possible values, either BEP or $(1-\mathrm{BEP})$. Because these two possibilities occur with the same frequency, (7) simplifies to:

$$C^\mathrm{4QAM} = 2\left[1 - H_b(\mathrm{BEP})\right], \tag{18}$$

with $H_b(\cdot)$ denoting the binary entropy function and BEP the uncoded bit error probability. Note that the expression inside the square brackets describes the capacity of a binary symmetric channel. Thus, for 4-QAM and perfect channel knowledge, our BICM system can be interpreted as transmitting bits over two identical binary symmetric channels. Applying Lemma 1 in (18), we finally get the simplified capacity expression as:

$$C^\mathrm{4QAM} = \frac{\log_2\left(\frac{2}{\sqrt{1+2\frac{1}{\mathrm{SNR}}}-1} + 1\right)}{\sqrt{1+2\frac{1}{\mathrm{SNR}}}} + \log_2\left(\frac{1}{1+\frac{1}{2}\mathrm{SNR}}\right). \tag{19}$$

For 4-QAM, the data symbols x have unit magnitude, so that the capacity for MMSE channel estimation can directly be obtained from the case of perfect channel knowledge, simply by decreasing the signal power and increasing the noise power according to (15):

$$C^\mathrm{4QAM,MMSE} = \left[\frac{\log_2\left(\frac{2}{\sqrt{1+2\frac{P_\mathrm{n}+\mathrm{MSE}}{P_\mathrm{s}-\mathrm{MSE}}}-1} + 1\right)}{\sqrt{1+2\frac{P_\mathrm{n}+\mathrm{MSE}}{P_\mathrm{s}-\mathrm{MSE}}}} + \log_2\left(\frac{1}{1+\frac{1}{2}\frac{P_\mathrm{s}-\mathrm{MSE}}{P_\mathrm{n}+\mathrm{MSE}}}\right)\right]. \tag{20}$$

Similar to the description above, we can straightforwardly find closed-form expressions for higher modulation orders by inserting Lemma 1 in (7). However, they consists of many summations and include $\tan^{-1}$ terms, making the closed-form expressions so large that we omit them at this point.

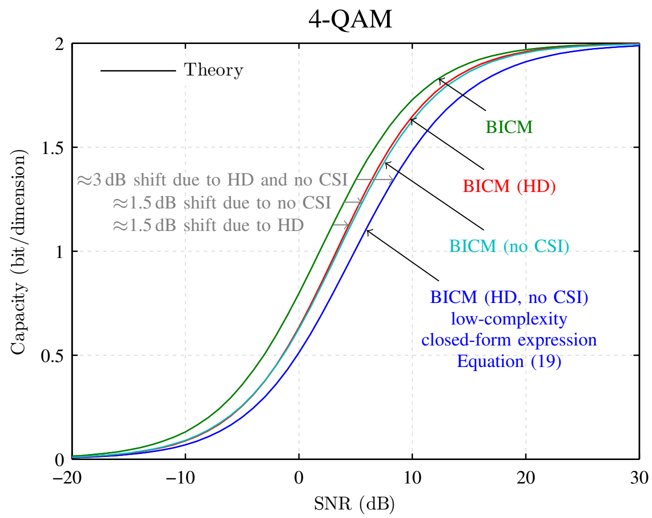

Fig. 2. When comparing our low-complexity closed-form capacity expression with the ordinary BICM capacity for **4-QAM**, we observe a 3 dB shift. Additionally we show how each of our main assumptions (hard decision and no CSI) affects the ordinary capacity.

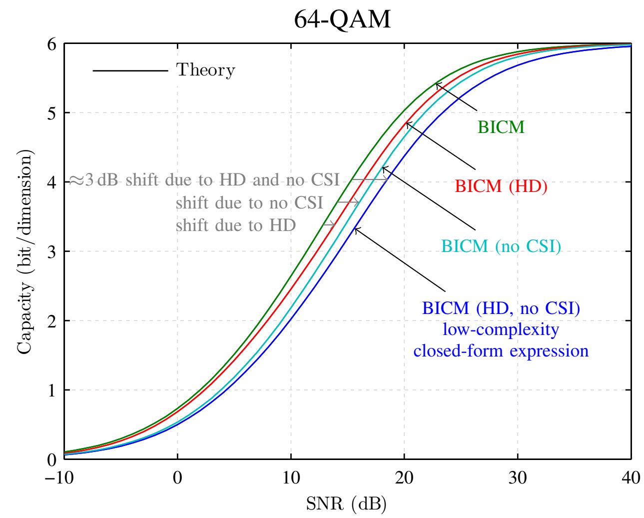

Fig. 3. When comparing our low-complexity closed-form capacity expression with the ordinary BICM capacity for **64-QAM**, we identify a 3 dB shift between these two curves. In contrast to Figure 2, the assumptions of hard decision and no CSI now lead to significantly different capacities.

IV. Capacity Comparison for Perfect Channel Knowledge

We now compare our closed-form capacity expression (7) with the ordinary BICM capacity (5) by using Monte Carlo evaluation for the latter. Additionally, we investigate the effect of our main assumptions (hard decision and no CSI) separately. Their corresponding capacities are given by:

$$C^{\text{HD}} = m - \sum_{i=1}^{m} \mathbb{E}_{b,\hat{x},h}\left[\log_2 \frac{\sum\limits_{x\in\mathcal{X}} \text{pmf}_h(\hat{x}|x)}{\sum\limits_{x\in\mathcal{X}_b^i} \text{pmf}_h(\hat{x}|x)}\right], \quad (21)$$

$$C^{\text{noCSI}} = m - \sum_{i=1}^{m} \mathbb{E}_{b,y}\left[\log_2 \frac{\sum\limits_{x\in\mathcal{X}} \text{pdf}(z|x)}{\sum\limits_{x\in\mathcal{X}_b^i} \text{pdf}(z|x)}\right]. \quad (22)$$

Note that the pmf in (21) can be expressed by Q-functions, the pdf in (22) can be found in [3] and the expectations $\mathbb{E}\{\cdot\}$ are evaluated by Monte Carlo simulation.

Figure 2 compares our closed-form capacity expression given by (19) with the usually considered BICM capacity for the case of 4-QAM. The curves are shifted by approximately 3 dB. Indeed, after a 3 dB shift, the error of our closed-form capacity expression relative to the ordinary BICM capacity is less than 3 % (calculated from the data points). The assumption of hard decision has a similar effect as the assumption of no CSI, i.e., it shifts the capacity by approximately 1.5 dB. Figure 3 depicts the case for 64-QAM. Again, our closed-form capacity expression is shifted by approximately 3 dB compared to the ordinary BICM capacity. To be specific, the relative error after a 3 dB shift is less than 2 % for SNRs larger than 10 dB. In contrast to 4-QAM, the assumptions of hard decision and no CSI now lead to significant different capacities. In particular, for a low SNR, the capacity C^{HD} approaches the ordinary capacity C^{BICM} because the 64 quantization levels provide enough information, while the capacity C^{noCSI} achieves our closed-form expression.

Up to now we assumed that the estimated data symbols $\hat{x}$ were chosen from the same set as the transmitted data symbols x, i.e., $\mathcal{X}$. Note that, by increasing the quantization steps in $\mathcal{Q}\{\cdot\}$, we can approach the capacity C^{noCSI} while maintaining the closed-form expression of our capacity. However, such method increases the overall complexity.

V. Testbed Measurement

In order to verify our system model and to show its applicability in real world true physical channels, we perform testbed measurements by using the Vienna Wireless Testbed [5], [6]. Our transmit antenna is located on the rooftop while the receive antenna is 130 m away and located indoor. We transmit an extended-cyclic-prefix LTE subframe which consists of 12 OFDM symbols and 24 subcarriers. Each of this 12×24 time-frequency resource elements can be modeled by our transmission system model (see Section II and Figure 1). The subcarrier spacing is set to 15 kHz and the carrier frequency is 2.5 GHz. We apply diamond shaped pilot symbols ($|\mathcal{P}| = 16$) as defined in the LTE standard.

We determine the **measured capacity** by estimating the pmf and inserting it in (7). To estimate the pmf, we transmit 1350 subframes whereas for each transmission the receive antenna is moved to another position within a 3×3 wavelength grid and to another azimuth angle within a range of 135°. Such relocation allows the evaluation of small-scale fading and, as it turns out, causes a channel h which is approximately Rayleigh distributed. Furthermore, we increase the accuracy of the estimated pmf by utilize symmetries of the pmf and averaging over all 12×24 resource elements. The latter is feasible because the delay spread as well as the Doppler spread are small so that all resource elements show approximately the same performance. We then repeat the whole procedure for different transmit power levels which relate to different SNR levels at the receiver.

The **theoretical capacity** is calculated by (7) in combination with Lemma 1. For the special case of 4-QAM, (19)

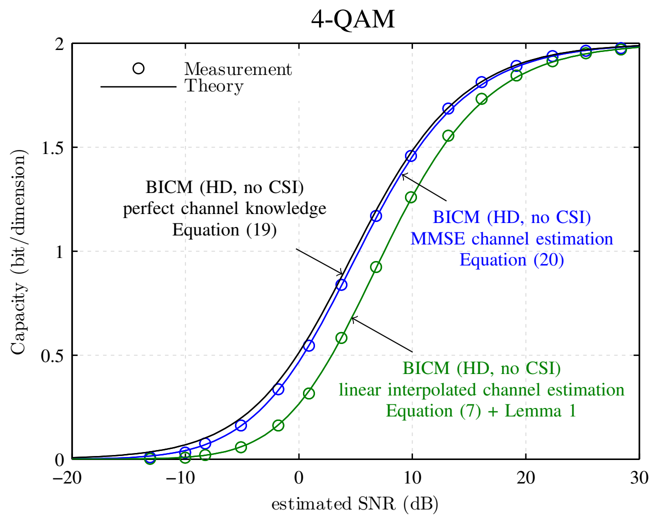

Fig. 4. Measurement results for **4-QAM**. The measured capacities and the theoretical capacities nearly perfectly overlap (within 0.02 bit/dim.), verifying our transmission system model. The performance of MMSE channel estimation comes close to perfect channel knowledge while for linear interpolated channel estimation we find a gap of approximately 2.5 dB.

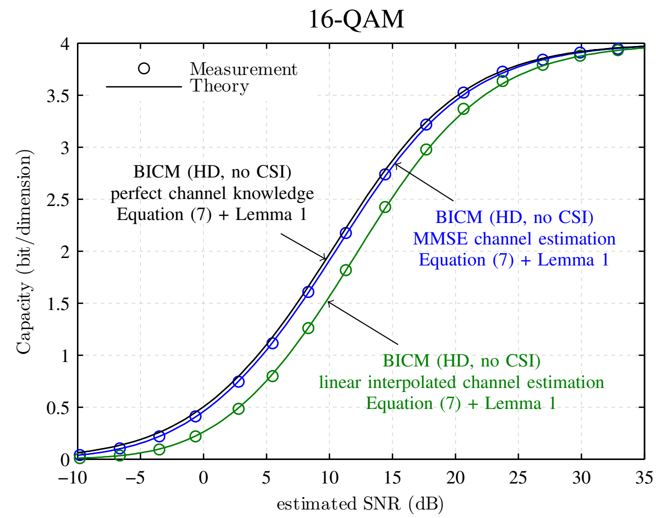

Fig. 5. Measurement results for **16-QAM**. The measured capacities and the theoretical capacities nearly perfectly overlap (within 0.03 bit/dim.), verifying our transmission system model. The performance of MMSE channel estimation comes close to perfect channel knowledge while for linear interpolated channel estimation we see a gap of approximately 2 dB.

and (20) provide simplified expressions. The only additional knowledge we need are the signal power, the noise power, the correlation vector $\mathbf{r}_{\hat{\mathbf{h}}_{\mathcal{P}}^{\mathrm{LS}},h}$ and the correlation matrix $\mathbf{R}_{\hat{\mathbf{h}}_{\mathcal{P}}^{\mathrm{LS}}}$, which are all estimated from the received signal. In particular the correlation matrix and vector are obtained by assuming a uniform power delay profile. By matching the theoretical (uniform power delay profile) and the measured correlation function we conclude that the maximum delay is 0.25 μs and that there are no Doppler shifts.

The results of our measurements are shown in Figure 4 and 5 where we see that the measured capacities coincide with the theoretical capacities. Thus, all relevant factors have been accurately included in our transmission system model. Furthermore, the MMSE channel estimation (12) comes close to the case of perfect channel knowledge because delay spread and Doppler spread are very low so that the channel for different time-frequency resource elements is highly correlated. On the other hand, for the linear interpolated channel estimation we identify a significant performance loss of approximately 2.5 dB for 4-QAM and 2 dB for 16-QAM.

VI. Conclusion

We derived closed-form expressions for the BICM capacity which are particularly useful for performance optimization with respect to a specific parameter. The derivation assumes quantization and no CSI at the decoder, which also reduces the decoding complexity. Compared to the ordinary BICM capacity, our closed-form expressions are shifted by approximately 3 dB. For 4-QAM, MMSE channel estimation shows the same performance as perfect channel knowledge except that the signal power is reduced by the MSE and the noise power increased by the MSE. For higher modulation orders we see a similar effect. Measurements conducted on the Vienna Wireless Testbed validate our closed-form expressions and show the applicability of our transmission system model in real world physical channels.

Acknowledgment

This work has been funded by the Christian Doppler Laboratory for Wireless Technologies for Sustainable Mobility, the A1 Telekom Austria AG, and the KATHREIN-Werke KG. The financial support by the Federal Ministry of Economy, Family and Youth and the National Foundation for Research, Technology and Development is gratefully acknowledged.

References

[1] G. Caire, G. Taricco, and E. Biglieri, “Bit-interleaved coded modulation,” *IEEE Transactions on Information Theory*, vol. 44, no. 3, pp. 927–946, 1998.

[2] A. G. i Fàbregas, A. Martinez, and G. Caire, *Bit-interleaved coded modulation*. Now Publishers Inc, 2008.

[3] R. Baxley, B. Walkenhorst, and G. Acosta-Marum, “Complex Gaussian ratio distribution with applications for error rate calculation in fading channels with imperfect CSI,” in *IEEE Global Telecommunications Conference (GLOBECOM)*, Miami, Florida, USA, Dec 2010.

[4] C. Novak and G. Matz, “Low-complexity MIMO-BICM receivers with imperfect channel state information: Capacity-based performance comparison,” in *IEEE Workshop on Signal Processing Advances in Wireless Communications (SPAWC)*, Marrakech, Morocco, June 2010.

[5] R. Nissel, M. Lerch, and M. Rupp, “Experimental validation of the OFDM bit error probability for a moving receive antenna,” in *IEEE Vehicular Technology Conference (VTC)*, Vancouver, Canada, Sept 2014.

[6] M. Lerch, S. Caban, M. Mayer, and M. Rupp, “The Vienna MIMO testbed: Evaluation of future mobile communication techniques.” *Intel Technology Journal*, vol. 4, pp. 58–69, 2014.

[7] A. G. i Fabregas and A. Martinez, “Bit-interleaved coded modulation with shaping,” in *IEEE Information Theory Workshop (ITW)*, 2010.

[8] D. Tse and P. Viswanath, *Fundamentals of wireless communication*. Cambridge university press, 2005.

[9] R. Nissel, M. Lerch, M. Šimko, and M. Rupp, “Bit error probability for pilot-symbol-aided OFDM channel estimation in doubly-selective channels,” in *18th International ITG Workshop on Smart Antennas (WSA)*, Erlangen, Germany, Mar 2014.

[10] R. Nissel and M. Rupp, “Doubly-selective MMSE channel estimation and ICI mitigation for OFDM systems,” in *IEEE International Conference on Communications (ICC)*, London, UK, June 2015.